AJNR

Enhancing Lesion Detection in Inflammatory Myelopathies: A Deep Learning – Reconstructed Double Inversion Recovery MRI Approach

Qiang Fang, Qing Yang, Bao Wang, Bing Wen, Guangrun Xu and Jingzhen He

AJNR Am J Neuroradiol 2025, 46 (6) 1180-1187
doi: https://doi.org/10.3174/ajnr.A8582
http://www.ajnr.org/content/46/6/1180

Enhancing Lesion Detection in Inflammatory Myelopathies: A Deep Learning–Reconstructed Double Inversion Recovery MRI Approach

Qiang Fang, Qing Yang, Bao Wang, Bing Wen, Guangrun Xu, and Jingzhen He

ABSTRACT

BACKGROUND AND PURPOSE: The imaging of inflammatory myelopathies has advanced significantly across time, with MRI techniques playing a pivotal role in enhancing lesion detection. However, the impact of deep learning (DL)-based reconstruction on 3D double inversion recovery (DIR) imaging for inflammatory myelopathies remains unassessed. This study aimed to compare the acquisition time, image quality, diagnostic confidence, and lesion detection rates among sagittal T2WI, standard DIR, and DL-reconstructed DIR in patients with inflammatory myelopathies.

MATERIALS AND METHODS: In this observational study, patients diagnosed with inflammatory myelopathies were recruited between June 2023 and March 2024. Each patient underwent sagittal conventional TSE sequences and standard 3D DIR (T2WI and standard 3D DIR were used as references for comparison), followed by an undersampled accelerated double inversion recovery deep learning (DIR_{DL}) examination. Three neuroradiologists evaluated the images using a 4-point Likert scale (from 1 to 4) for overall image quality, perceived SNR, sharpness, artifacts, and diagnostic confidence. The acquisition times and lesion detection rates were also compared among the acquisition protocols.

RESULTS: A total of 149 participants were evaluated (mean age, 40.6 [SD, 16.8] years; 71 women). The median acquisition time for DIR_{DL} was significantly lower than for standard DIR (298 seconds [interquartile range, 288–301 seconds] versus 151 seconds [interquartile range, 148–155 seconds]; $P < .001$), showing a 49% time reduction. DIR_{DL} images scored higher in overall quality, perceived SNR, and artifact noise reduction (all $P < .001$). There were no significant differences in sharpness ($P = .07$) or diagnostic confidence ($P = .06$) between the standard DIR and DIR_{DL} protocols. Additionally, DIR_{DL} detected 37% more lesions compared with T2WI (300 versus 219; $P < .001$).

CONCLUSIONS: DIR_{DL} significantly reduces acquisition time and improves image quality compared with standard DIR, without compromising diagnostic confidence. Additionally, DIR_{DL} enhances lesion detection in patients with inflammatory myelopathies, making it a valuable tool in clinical practice. These findings underscore the potential for incorporating DIR_{DL} into future imaging guidelines.

ABBREVIATIONS: AQP4+NMOSD = AQP4-IgG positive neuromyelitis optica spectrum disorders; DIR = double inversion recovery; DL = deep learning; ICC = intraclass correlation coefficient; IQR = interquartile range; MOG = myelin oligodendrocyte glycoprotein; MOGAD = MOG antibody-associated diseases; NEX = number of excitations

Since the seminal work of Devic in the late 19th century describing neuromyelitis optica, our understanding and imaging techniques for inflammatory myelopathies have evolved significantly. Inflammatory myelopathies are immune-mediated inflammations of the spinal cord, often seen in conditions like MS, AQP4-IgG-positive neuromyelitis optica spectrum disorders (AQP4+NMOSD), and myelin oligondendrocyte glycoprotein (MOG) antibody-associated diseases (MOGAD).[1,2] Symptoms typically include limb weakness and sensory abnormalities.[3,4] MRI is essential for diagnosing inflammatory spinal cord lesions.[5-7] However, conventional MRI sequences may show negative results in the early disease stages or when lesions are small.

The double inversion recovery (DIR) sequence uses 2 inversion pulses to significantly suppress signals from CSF and white matter. This technique enhances the contrast between gray and white matter, thereby improving delineation.[8,9] DIR is primarily used for visualizing intracranial lesions, especially in cortical regions.[10-14] However, the small size of the spinal cord, combined with artifacts from swallowing, respiration, cardiac pulsation, and

Received September 7, 2024; accepted after revision November 9.

From the Departments of Radiology (Q.F., Q.Y., B. Wang, J.H.) and Neurology (B. Wen, G.X.), Qilu Hospital of Shandong University, Jinan, Shandong Province, China.

Qiang Fang and Qing Yang contributed equally to this work and should be considered as co-first authors.

This work was supported by the Shandong Provincial Natural Science Foundation (ZR2021MH237) and the National Natural Science Foundation of China (82202114).

Please address correspondence to Jingzhen He, MD, Department of Radiology, Qilu Hospital of Shandong University, No. 107 West Wenhua Rd, Jinan, Shandong Province, 250012, China; e-mail: hjzhhjzh@163.com

Indicates article with supplemental data.

http://dx.doi.org/10.3174/ajnr.A8582

SUMMARY

PREVIOUS LITERATURE: DL-based MRI reconstruction techniques have shown promise in reducing scan times and enhancing image quality across various applications, including musculoskeletal imaging and the CNS. DIR sequences, particularly effective in identifying lesions in MS, have been primarily applied for brain imaging, with limited use in spinal cord assessments. Prior studies have explored the ability of DIR to improve lesion detection by suppressing signals from CSF and white matter, but there were challenges with artifacts, and long scan times remain. The application of DL techniques to DIR sequences represents a novel solution to these issues.

KEY FINDINGS: The study demonstrated that DIR_{DL} significantly reduced acquisition time by 49.33% while enhancing image quality. Additionally, DIR_{DL} improved lesion detection by 36% compared with standard T2WI, showing superior diagnostic performance in inflammatory myelopathies without compromising diagnostic confidence.

KNOWLEDGE ADVANCEMENT: This research advances the integration of DL with DIR sequences, optimizing spinal cord lesion detection. By significantly reducing scan time and improving image quality, the DIR_{DL} technique offers the potential for broader clinical adoption, particularly in enhancing diagnosis and patient throughput in cases of inflammatory myelopathies.

longer scan times, degrades image quality and lowers diagnostic confidence. Currently, to the best of our knowledge, DIR sequences for the entire spinal cord are not well-established in clinical practice or research. Only a few studies have reported their application, primarily focusing on the cervical spinal cord in conditions such as MS and related inflammatory diseases.[15-17] Deep learning (DL)-based MRI reconstructions have emerged as a transformative approach in medical imaging. Techniques such as end-to-end reconstruction, UNet-based methods, and Generative Adversarial Networks are widely used. By integrating DL algorithms with traditional physical principles, these methods aim to enhance reconstruction quality by accelerating acquisition, reducing artifacts, and improving overall image clarity.[18-21]

Therefore, this study aimed to compare the acquisition time, image quality, and diagnostic confidence between DL-reconstructed DIR (DIR_{DL}) and conventional DIR in patients with inflammatory myelopathies.

MATERIALS AND METHODS

Study Participants

This single-center, observational study was conducted with approval from the Ethical Review Committee of Qilu Hospital of Shandong University. All procedures conformed rigorously to the ethical standards in the 1964 Declaration of Helsinki and its later amendments. Participation in the study was voluntary, and all participants provided written informed consent. Our study adheres to the methodology outlined in the Standards for the Reporting of Diagnostic Accuracy Studies (STARD) checklist.

Patients diagnosed with inflammatory myelopathies between June 2023 and March 2024 were included in the study. MRI scans were performed on all patients within 3 days following their admission to the hospital. Inclusion criteria were the following: 1) the presence of typical clinical symptoms, including limb weakness and sensory abnormalities; and 2) supportive laboratory findings, including CSF examination and blood tests. Exclusion criteria were the presence of contraindications to MRI, including pacemakers, severe claustrophobia, any previous spinal surgery, and poor image quality due to patient movement.

Imaging Protocol

All MRI examinations were performed using a 3T MRI scanner (Signa Architect; GE Healthcare). Each participant underwent fast recovery fast spin-echo T2WI, conventional DIR, and DIR_{DL} sequences. The localization of DIR and DIR_{DL} sequences was copied from the T2WI sequence to ensure accurate comparison. The detailed MRI sequence parameters can be found in Table 1.

The DL reconstruction software (AIR Recon DL; GE Healthcare) uses a deep convolutional neural network algorithm designed for processing raw *k*-space data. Operating in the complex domain, it effectively reduces noise and mitigates artifacts such as Gibbs artifacts. Furthermore, the software enhances image sharpness by extrapolating truncated high-frequency *k*-space data. It offers adjustable noise reduction capabilities, with a setting of 75% used in this study. The acquisition times of the T2WI, DIR, and DIR_{DL} sequences were documented for comparative analysis.

Table 1: MRI sequence parameters

Parameter	T2WI	DIR	DIR_{DL}
Field of view (mm × mm)	300 × 225	300 × 225	300 × 225
Matrix	260 × 224	200 × 200	200 × 200
Slice thickness (mm)	3.00	1.50	1.50
Acquisition voxel size (mm)	0.6 × 0.7 × 3.0	1.5 × 1.5 × 1.5	1.5 × 1.5 × 1.5
Acceleration phase	2.00	2.00	2.00
Echo spacing (ms)	5.7	5.5	5.7
TR (ms)	5000	7000	7000
TE (ms)	90	90	90
TI (ms)	/	2884/546[a]	2884/546[a]
NEX	2.00	2.00	1.00
Bandwidth/pixel (Hz)	641.0	357.1	357.1
Acquisition time (minutes:seconds)	2:25	4:58	2:31

[a] The long TI1 (2884 ms) is defined as the interval between the first 180° inversion pulse and the 90° excitation pulse. The short inversion time TI2 (546 ms) is defined as the interval between the second 180° inversion pulse and the 90° excitation pulse.

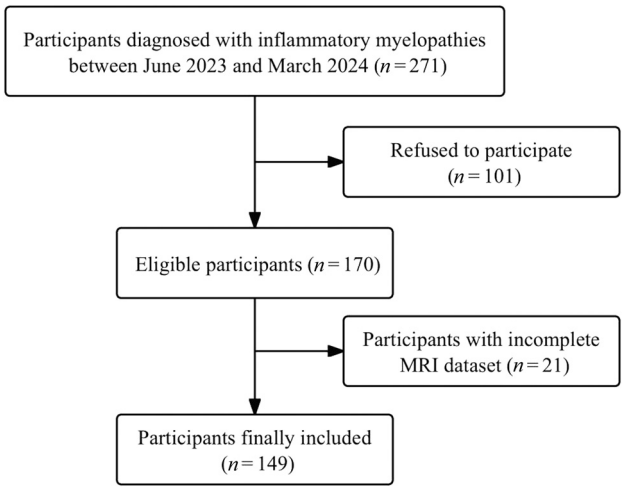

FIG 1. Flow chart of participant inclusion and exclusion.

Table 2: Epidemiologic data of patients with inflammatory myelopathies[a]

Characteristic	Value
No.	149
Sex	
Male	78 (52%)
Female	71 (48%)
Age (mean) (yr)	40.6 (SD, 16.8) (18–89)
Body mass index (mean)	24.5 (SD, 5.3)
Primary symptoms (mean)	
Progressive weakness and spasticity	32 (22%)
Hemiparesis/paraparesis/quadriparesis	78 (52%)
Sensory deficits or ataxia	31 (21%)
Bowel or bladder dysfunction	8 (5.4%)
Types of myelitis	
MS	85 (57%)
AQP4+NMOSD	26 (17%)
MOGAD	16 (11%)
Anti-GFAP astrocytopathy	10 (6.7%)
Paraneoplastic myelopathies	8 (5.4%)
Acute disseminated encephalomyelitis	3 (2.0%)
Behçet disease	1 (0.7%)

Note:—GFAP indicates glial fibrillary acidic protein.
[a] The total number of patients is 149. Data in parentheses are ranges. Body mass index is calculated by kilograms of body weight per meters of height squared.

Image Analysis

Each examination was independently evaluated by 3 board-certified neuroradiologists with 8–26 years of subspecialty experience. Reviewers were blinded to all clinical data to ensure unbiased assessments. Intrarater reliability was assessed using intraclass correlation coefficients (ICCs), with a 4-week washout period between image reviews to minimize recall bias. The randomization of image order was performed using a computer-generated randomization sequence. Readers viewed images without participant or sequence-identifying markers and were blinded to reconstruction type, radiologic reports, and other readers' evaluations. A dedicated PACS workstation (AGFA IMPAX Image Viewer, Version 6.5; AGFA Healthcare) was used for image analysis under certified reading room conditions.

First, each reader using an adapted semiquantitative 4-point Likert scale evaluated DIR and DIR_{DL} images from the following aspects: overall image quality (1: poor, 2: moderate, 3: good, 4: excellent), perceived SNR (1: poor, 2: moderate, 3: good, 4: excellent), sharpness of the anatomic structures (1: poor, 2: moderate, 3: good, 4: excellent), and diagnostic confidence (1: inadequate assessment of any pathologies; 2: lesion detection still possible, moderate suspicion of a lesion; 3: good lesion detection with a high suspicion of a lesion; 4: excellent lesion detection with a very high suspicion of a lesion). Artifacts were evaluated as 1: severe; 2: moderate; 3: mild; and 4: none.

Then, we evaluated several specific features of the lesions and surrounding structures on DIR and DIR_{DL} images. These features included location, single or multiple lesions, length, morphology, focal cord swelling, focal cord atrophy, and central canal involvement. The frequency of each pathologic feature in each data set was calculated and compared. Additionally, interchangeability, agreement, and concordance analyses were performed on these features. Equivalence indices were calculated to assess the agreement between DIR and DIR_{DL} protocols across these key imaging parameters. Finally, we analyzed the lesion load measurement in patients with MS by counting the number of lesions in different spinal cord locations on T2WI, DIR, and DIR_{DL} images.

Statistical Analysis

The sample size was calculated on the basis of an effect size of 0.5, a significance level (α) of .05, and a power of 0.80. The Kolmogorov-Smirnov test was used to determine if the data adhered to a normal distribution. The Wilcoxon signed-rank test was used to compare the image-quality scores and conduct subgroup analyses between DIR and DIR_{DL}. The image-quality interpretation between the 2 data sets for each reader in the same participant was compared. The McNemar test was used to analyze the differences in the frequency of major pathologic features and to conduct power analysis. ICCs were used to assess the reliability of ratings. The Kendall τ (τ) and Kendall coefficient of concordance were used to assess the degree of concordance. Agreement was evaluated using weighted Fleiss κ (κ) values and ICCs. The strength of agreement for κ values was categorized as follows: <0.20, poor; 0.21–0.40, fair; 0.41–0.60, moderate; 0.61–0.80, substantial; and 0.81–1.00, almost perfect agreement.[22] A P value $< .05$ was considered a statistically significant difference. Statistical analysis was performed using Matlab software (Version 2021a; MathWorks) and SPSS (Version 20; IBM).

RESULTS

Participant Characteristics

In this prospective study, 149 participants diagnosed with inflammatory myelopathies were enrolled (mean age, 40.6 [SD, 16.8] years; 71 women). The calculated sample size was 126 participants. Of 271 eligible patients, 101 declined to participate, and 21 were excluded due to incomplete MRI data sets (Fig 1). Table 2 presents the demographics of the study participants, including age, sex, primary symptoms, and various types of myelitis.

Acquisition Time

The acquisition times for the MRI sequences were as follows: The median scan time for the T2WI sequence was 145 seconds (interquartile range [IQR], 138–150 seconds; range, 138–155 seconds);

Table 3: Intraprotocol reader agreement between standard DIR MRI, interprotocol reader agreement between DIR_{DL} and standard DIR MRI, and the individual equivalence index

Variable	Intraprotocol Assessment (447 Pair-Wise Comparisons)		Interprotocol Assessment (2235 Pair-Wise Comparisons)		Individual Equivalence Index (%)
	No. of Examinations	Agreement (%)	No. of Examinations	Agreement (%)	
Location	431	96.4	2179	97.5	−0.3 (−0.8–1.4)
Single or multiple	437	97.8	2190	98.0	0.1 (−0.6–0.5)
Length	439	98.2	2070	92.6	−0.2 (−1.0–1.2)
Morphology	411	92.0	2007	89.8	−0.1 (−0.9–1.1)
Focal cord swelling	427	95.5	2177	97.4	0.2 (−1.1–0.7)
Focal cord atrophy	430	96.2	2166	96.9	0.1 (−0.5–0.6)
Central canal involvement	443	99.1	2208	98.8	−0.1 (−0.7–0.9)

Note:—Data in parentheses are 95% CIs. The test of interchangeability is as follows: Intraprotocol agreement is the agreement between 2 readers independently reviewing images from the same participant using the standard DIR protocol. Interprotocol agreement is the agreement between 2 readers independently reviewing images from the same participant using both the standard DIR and DIR_{DL} protocols. Three readers reviewed the images, resulting in 3 reader pairs for intraprotocol analysis and 15 reader pairs for interprotocol analysis, yielding 447 comparisons (149 MRI examinations ×3 pairs) for intraprotocol and 2235 comparisons (149 examinations ×15 pairs) for interprotocol analyses.

Table 4: Comparison of image quality and diagnostic confidence between standard DIR and DIR_{DL} MRI

Parameter Assessed	Mean DIR Score (SD)	Mean DIR_{DL} Score (SD)	Kendall τ[a]	ICC[b]	*P* Value[c]
Overall image quality	3.7 (0.5)	4.1 (0.4)	0.31	0.33	<.001
Perceived SNR	3.6 (0.6)	4.0 (0.3)	0.09	0.08	<.001
Sharpness	3.8 (0.4)	4.2 (0.3)	0.61	0.64	.07
Artifacts	3.9 (0.5)	4.3 (0.3)	0.43	0.49	<.001
Diagnostic confidence	3.9 (0.5)	4.2 (0.4)	0.79	0.78	.06

Note:—Data in parentheses are SDs. Each parameter was assessed by 3 readers on 149 spine MRI scans using a 4-point Likert scale, with a score of 4 indicating excellence and a score of 1 indicating inadequacy.
[a] Kendall rank correlation coefficients assess the correlation between scores assigned to standard DIR and DIR_{DL}.
[b] Two-way mixed model assesses absolute agreement between scores assigned to standard DIR and DIR_{DL}.
[c] Wilcoxon signed-rank test compares scores between standard DIR and DIR_{DL}.

for the standard DIR sequence, it was 298 seconds (IQR, 288–301 seconds; range, 288–312 seconds); and for the DIR_{DL} sequence, it was 151 seconds (IQR, 148–155 seconds; range, 148–167 seconds). The median acquisition time for DIR_{DL} was significantly lower than that of standard DIR ($P < .001$), representing a 49% reduction in scan time.

Interreader Agreement and Equivalence Analysis of Standard DIR and DIR_{DL} MRI

The interreader agreement of the DIR_{DL} and standard DIR showed no significant difference compared with that of standard DIR alone, with all individual equivalence indexes falling within ±1.5%. Specifically, the maximum disagreement was observed for the location variable at −0.3% (95% CI, −0.82−1.41). For all other variables, the absolute individual equivalence indexes were ≤0.2%. Both the intraprotocol (DIR versus DIR) and interprotocol (DIR versus DIR_{DL}) reader agreements were high, with agreement percentages ranging from 89.8% to 99.1%. The intraprotocol assessment based on 447 pair-wise comparisons showed agreement percentages ranging from 92.0% to 99.1% across all variables. Similarly, the interprotocol assessment, involving 2235 pair-wise comparisons, demonstrated agreement percentages ranging from 89.8% to 98.8%. The highest agreement was observed for central canal involvement in both assessments (99.1% for intraprotocol and 98.8% for interprotocol), while morphology showed the lowest agreement (92.0% for intraprotocol and 89.8% for interprotocol). These results suggest that DIR_{DL} provides diagnostic information comparable with that of standard DIR MRI across various imaging parameters. For detailed results, please refer to Table 3.

Image Quality and Diagnostic Confidence

In this study, the DIR_{DL} images consistently outperformed the standard DIR images across multiple parameters. Table 4 demonstrates that the median scores for overall image quality, perceived SNR, sharpness, artifact presence, and diagnostic confidence were higher for DIR_{DL} compared with standard DIR. The median overall image-quality score for DIR_{DL} was 4 (IQR, 4–4) compared with 4 (IQR, 3–4) for standard DIR, with a significant P value <.01. Similarly, perceived SNR and artifact scores were significantly better in DIR_{DL} (both $P < .01$). An example can be seen in Fig 2. Although the sharpness score did not show a significant difference ($P = .07$), the diagnostic confidence score was notably higher for DIR_{DL} ($P = .06$). The ICCs and Kendall rank correlation coefficients confirmed the significant improvements in image quality and diagnostic confidence with DIR_{DL}. Comprehensive results can be found in Table 4.

Lesion-Detection Rate in MS

The lesion-detection rates differed among T2WI, DIR, and DIR_{DL} in 85 cases of MS across the cervical, thoracic, and lumbar spinal cord regions. In the cervical region, DIR and DIR_{DL} both detected 168 lesions compared with 129 with T2WI, representing a 30% higher detection rate (39 additional lesions). In the thoracic region, DIR and DIR_{DL} detected 110 lesions each, compared with 78 with T2WI, indicating a 41% higher detection rate (32 additional lesions). In the lumbar region, DIR and DIR_{DL} respectively detected 21 and 22 lesions, compared with 12 with T2WI, resulting in a 75% and 83% higher detection rate (9 and 10 additional lesions). Overall, DIR and DIR_{DL} exhibited a 36% higher lesion-detection rate compared with T2WI. These differences are statistically significant ($P < .001$). Detailed data

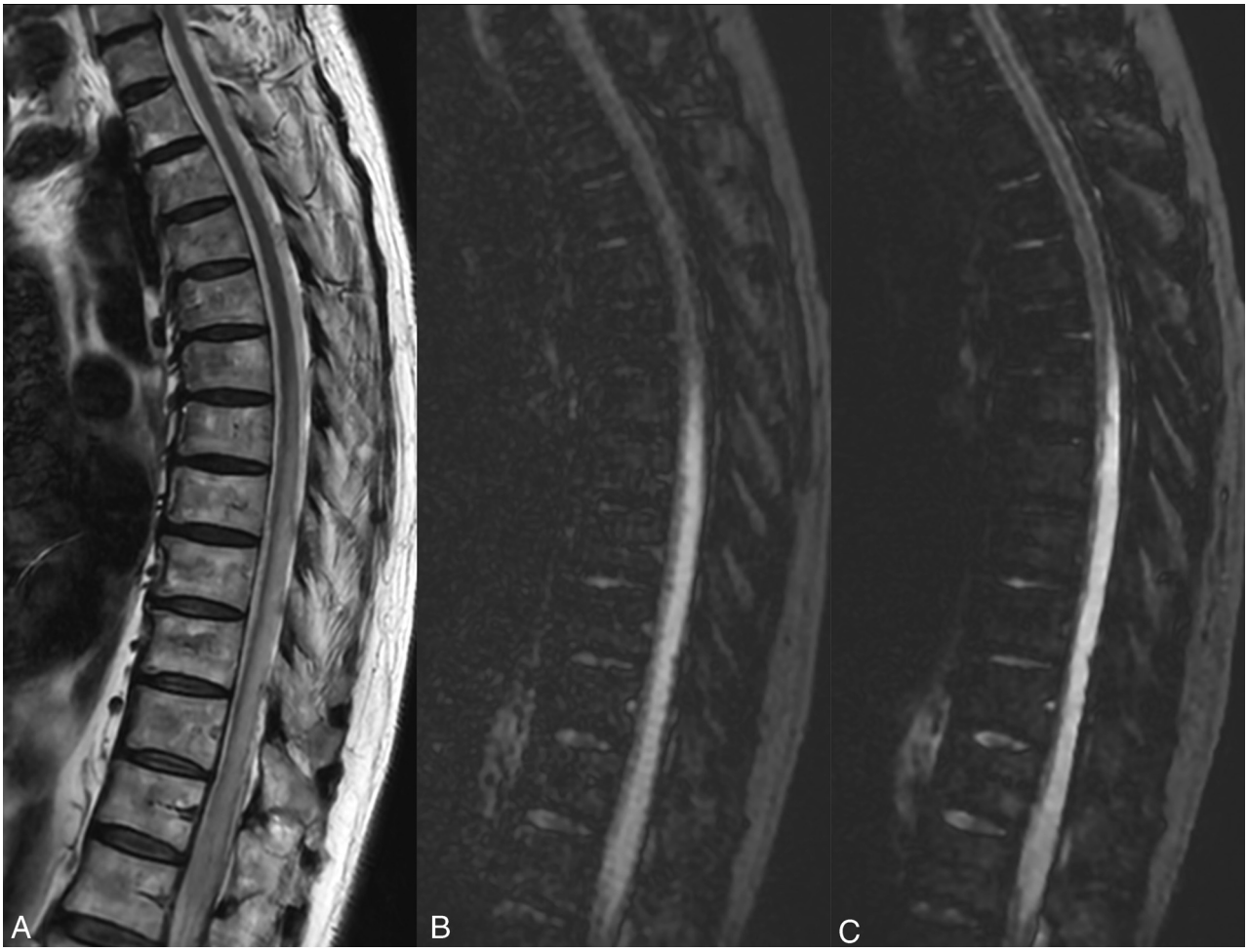

FIG 2. Sagittal thoracic spinal cord MR images of a 45-year-old man with MOGAD are presented. T2WI (*A*), DIR (*B*), and DIR_{DL} (*C*). Long segments of high signal in the thoracolumbar spinal cord are clearly visible in all sequences, with greater clarity observed in the conventional DIR and DIR_{DL} images. DIR_{DL} images demonstrate a higher perceived SNR and improved overall image quality.

Table 5: Analysis of lesion load measurement and relative comparisons of DIR_{DL}, DIR, and T_2WI sequences in 85 cases of MS

Region	T2WI[b]	DIR[b]	DIR_{DL}[b]	Relative Comparison (%)[a]			
				DIR_{DL}/T2WI	*P* Value[c]	DIR_{DL}/DIR	*P* Value[c]
Cervical spinal cord	129	168	168	30	.04	0	.95
Thoracic spinal cord	78	110	110	41	.03	0	.89
Lumbar spinal cord	12	21	22	83	.01	5	.95
Total	219	299	300	36	.008	0	.91

[a] Data are relative differences in the numbers of detected lesions expressed as percentages of lesion numbers identified with DIR_{DL} imaging compared with the corresponding T2WI and DIR.
[b] Data are the number of detected lesions.
[c] The *P* value was obtained from the patient-wise Wilcoxon analysis for matched pairs indicating that more or fewer patients showed higher lesion load measurement with DIR_{DL} imaging compared with the corresponding T2WI and DIR imaging.

are available in Table 5. Figure 3 illustrates the display differences of MS in various sequences for a single case.

DISCUSSION

DL-based MRI reconstructions can reduce examination times for DIR scans. This study found that the DIR_{DL} technique, compared with standard DIR, resulted in a roughly 49% decrease in examination duration. It also enhanced overall image quality, indicated by higher Likert scale scores (median score, 4 [IQR, 3–4] versus 4 [IQR, 4–4]), better-perceived SNR (median score, 4 [IQR, 4–4 versus IQR, 3–4]), and fewer artifacts (median score: 4 [IQR, 3–4] versus 4 [IQR, 4–4]) (all, $P < .01$). Furthermore, the DIR_{DL} demonstrated a 36% increase in the lesion-detection rate compared with T2WI ($P < .001$).

Inflammatory myelopathies, which refer to spinal cord inflammation, can occur in various immune-mediated disorders. MS represents the leading cause of inflammatory myelopathy and is characterized by spatial and temporal dissemination. On T2WI,

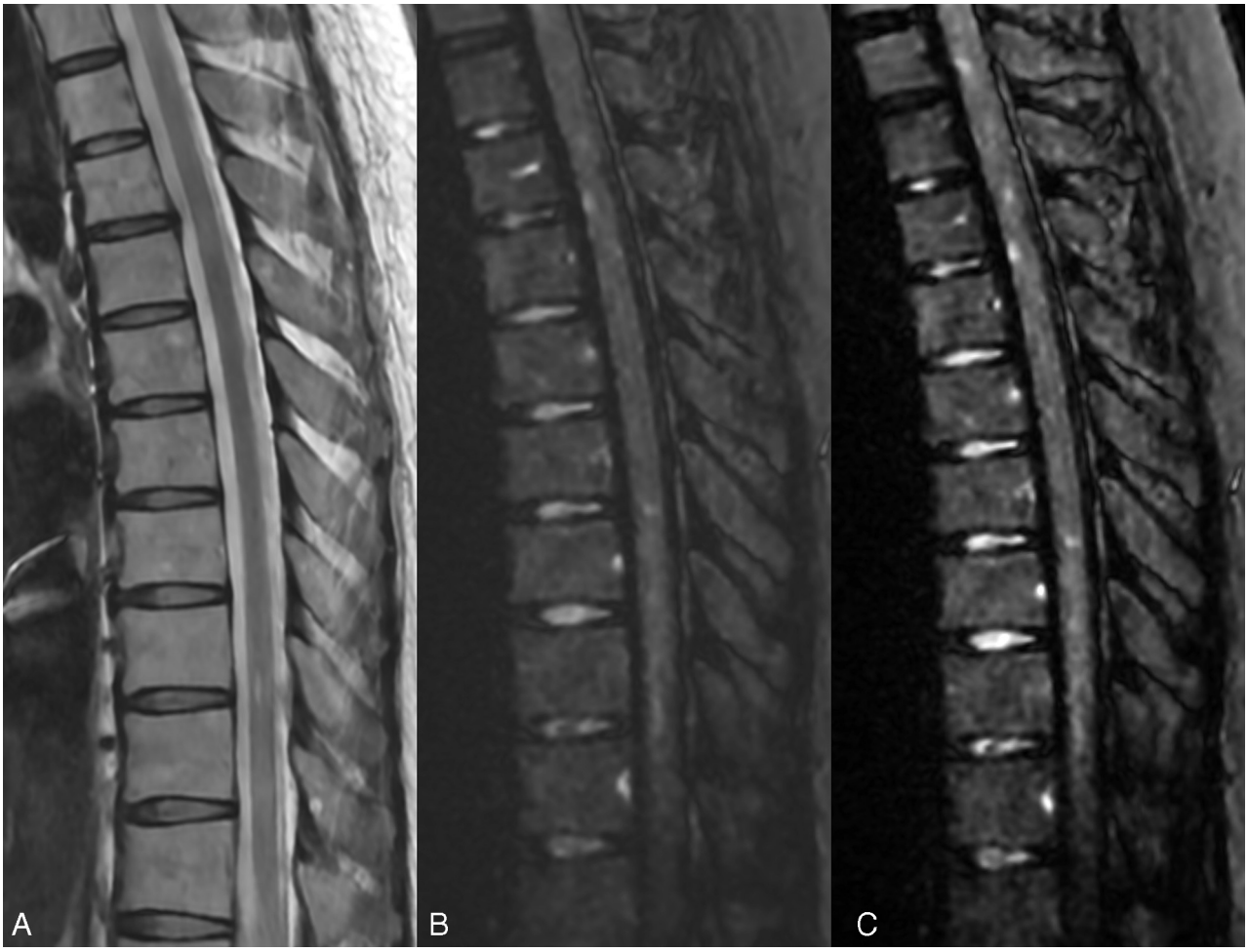

FIG 3. Sagittal thoracic spinal cord MR images of a 36-year-old woman diagnosed with MS. T2WI (*A*), conventional DIR (*B*), and DIR_{DL} (*C*). On T2WI, only a single short linear high signal is visible, while on DIR and DIR_{DL}, multiple punctate and short linear high signals can be seen. The lesions are displayed more clearly on DIR_{DL}.

MS typically presents as slightly hyperintense, while on DIR sequences, it appears as distinctly hyperintense, with or without surrounding edema. Some small lesions may not be clearly visible on conventional sequences. Therefore, we chose MS to compare the detection rates between DIR and T2WI sequences. Our results are consistent with previous literature,[10-12,14] indicating that the DIR sequence can detect more lesions in MS. The DL-based reconstruction algorithm used in this study, AIRTM Recon DL (GE Healthcare), uses convolutional neural networks to process raw *k*-space data and significantly reduces noise and artifact levels. Evaluating the trustworthiness of DL-generated images is critical, particularly in clinical settings. This evaluation can be achieved through rigorous assessment of reader agreement and concordance analysis, which, in this study, demonstrated high interreader and intrareader reliability, indicating the reproducibility and reliability of DL-generated images.

The results of this study align with the earlier findings of Almansour et al[19] and Herrmann et al.[22,23] Specifically, DL-reconstructed MRI acquisitions demonstrated excellent image quality and significantly reduced acquisition time. Their studies primarily evaluated the feasibility of TSE_{DL} technology in routine clinical practice for musculoskeletal applications, including the spine, shoulder, wrist, and hand. Our study expands on these findings by integrating previous research and simultaneously applying both DIR and DL techniques. This combination supports the interchangeability of DIR_{DL} and standard DIR results in the imaging of inflammatory myelopathies, building on the foundations of previous scholars.[16,21] While DIR sequences are not yet part of the current consensus guidelines for spinal cord imaging in demyelinating diseases, their utility is increasingly supported by emerging research. International consensus documents, such as those from the MAGNIMS-CMSC-NAIMS group,[7] play a critical role in standardizing imaging practices across institutions and countries to ensure consistent patient care and diagnosis. The role of DIR, and specifically DL-enhanced DIR, should be considered as part of future revisions of these guidelines due to its ability to enhance lesion detection and reduce acquisition time. As more studies validate the use of DL DIR in diverse patient populations, it is likely that these techniques will become integral to routine clinical practice, providing a more efficient and effective diagnostic tool for inflammatory myelopathies.

The current diagnosis of spinal cord lesions still primarily relies on traditional multisequence MR imaging protocols. For inflammatory myelopathies, the MRI diagnosis should not be

limited to qualitative analysis; details such as lesion location, number, and involvement of gray or white matter are more crucial because they will influence patient management and prognosis.[24,25] In this study, we introduced the DIR sequence, which effectively attenuates CSF and white matter. This addition leads to an improved contrast ratio and clearer delineation between gray and white matter compared with T2 TSE imaging, enabling a more detailed display of lesion characteristics. However, the scan time is relatively long. The integration of DL-based MRI reconstruction techniques with traditional DIR sequences effectively addresses the issue of long scan times. Additionally, DIR_{DL} generally enhances image quality, ensuring that radiologists maintain diagnostic confidence. This study confirms this. In clinical practice, the reduction in acquisition time without compromising image quality can significantly enhance patient throughput, reducing wait times and increasing the availability of MRI scanners for a broader patient population. This efficiency gain is particularly beneficial in busy hospital environments where the demand for MRI scans often exceeds capacity. Moreover, faster acquisition times can improve patient comfort, especially for those who experience anxiety or discomfort during prolonged MRI procedures.

From a research standpoint, the rapid acquisition of high-quality images precedes investigating dynamic processes and performing longitudinal studies. The superior image quality enabled by DL reconstruction algorithms guarantees that subtle anatomic and pathologic details are portrayed, crucial for precise diagnosis and research outcomes. Furthermore, shorter scan times allow more comprehensive data collection within the same period, enhancing the robustness and statistical power of studies. Ongoing enhancements in DL algorithms, fueled by the growing availability of large data sets and computational resources, are expected to further improve image quality and shorten acquisition times. Such progress may also result in the development of novel imaging protocols tailored to specific clinical or research requirements, further expanding the applications of MRI technology.

Although DIR_{DL} significantly reduced acquisition time, further analysis suggests that the reduction in the number of excitations (NEX) may independently affect lesion detection and image quality. Because DIR_{DL} combines both the reduced NEX and DL-based reconstruction, it remains unclear to what extent the DL algorithm alone contributed to the observed improvements. Including a control arm that compares DIR sequences with reduced NEX but without DL reconstruction could have provided clearer insight into this distinction. Future studies should incorporate such a control arm to more precisely evaluate the individual contributions of reduced NEX and the DL algorithm to the observed improvements in image quality and lesion detection.

This study has limitations. First, the study was conducted at a single center with a relatively small sample size, possibly limiting the generalizability of the findings. Second, our study focused on unenhanced DIR imaging and did not compare it with T1-weighted contrast-enhanced imaging, nor did we measure the specific volume of the lesions. Future research should be conducted to address these issues. Third, this study did not include postoperative spine patients, so the artifacts generated by metal implants in the DIR_{DL} sequence were not evaluated. Finally, while the consecutive inclusion of cases reduced selection bias, the limitation remains that the included cases had obvious pathologic features, resulting in high reader agreement.

CONCLUSIONS

This study demonstrates that DIR_{DL} significantly reduces acquisition time and enhances image quality compared with standard DIR, without compromising diagnostic confidence. These features make DIR_{DL} a valuable tool in the clinical evaluation of inflammatory myelopathies. Further research, particularly multicenter studies, is necessary to confirm these findings and promote the broader adoption of DIR_{DL} in clinical practice.

ACKNOWLEDGMENTS

We thank Dr Tianyong Xu from GE Healthcare for his assistance with the manuscript revisions and editorial suggestions.

Disclosure forms provided by the authors are available with the full text and PDF of this article at www.ajnr.org.

REFERENCES

1. Cacciaguerra L, Sechi E, Rocca MA, et al. **Neuroimaging features in inflammatory myelopathies: a review.** *Front Neurol* 2022;13:993645 CrossRef Medline
2. Lopez Chiriboga S, Flanagan EP. **Myelitis and other autoimmune myelopathies.** *Continuum (Minneap Minn)* 2021;27:62–92 CrossRef
3. Douglas AG, Xu DJ, Shah MP. **Approach to myelopathy and myelitis.** *Neurol Clin* 2022;40:133–56 CrossRef Medline
4. Fadda G, Flanagan EP, Cacciaguerra L, et al. **Myelitis features and outcomes in CNS demyelinating disorders: comparison between multiple sclerosis, MOGAD, and AQP4-IgG-positive NMOSD.** *Front Neurol* 2022;13:1011579 CrossRef Medline
5. Bulut E, Shoemaker T, Karakaya J, et al. **MRI predictors of recurrence and outcome after acute transverse myelitis of unidentified etiology.** *AJNR Am J Neuroradiol* 2019;40:1427–32 CrossRef Medline
6. Mustafa R, Passe TJ, Lopez-Chiriboga AS, et al. **Utility of MRI enhancement pattern in myelopathies with longitudinally extensive T2 lesions.** *Neur Clin Pract* 2021;11:e601–11 CrossRef Medline
7. Wattjes MP, Ciccarelli O, Reich DS, et al. **2021 MAGNIMS–CMSC–NAIMS consensus recommendations on the use of MRI in patients with multiple sclerosis**. *Lancet Neurol* 2021;20:653–70 CrossRef
8. Redpath TW, Smith FW. **Technical note: use of a double inversion recovery pulse sequence to image selectively grey or white brain matter.** *Br J Radiol* 1994;67:1258–63 CrossRef Medline
9. Saranathan M, Worters PW, Rettmann DW, et al. **Physics for clinicians: fluid-attenuated inversion recovery (FLAIR) and double inversion recovery (DIR) imaging**. *J Magn Reson Imaging* 2017; 46:1590–600 CrossRef Medline
10. Costagli M, Lapucci C, Zacà D, et al. **Improved detection of multiple sclerosis lesions with T2-prepared double inversion recovery at 3T**. *J Neuroimaging* 2022;32:902–09 CrossRef Medline
11. Martin A, Emorine T, Megdiche I, et al. **Accurate diagnosis of cortical and infratentorial lesions in multiple sclerosis using accelerated fluid and white matter suppression imaging.** *Invest Radiol* 2023; 58:337–45 CrossRef Medline
12. Bouman PM, Strijbis VI, Jonkman LE, et al. **Artificial double inversion recovery images for (juxta)cortical lesion visualization in multiple sclerosis.** *Mult Scler* 2022;28:54–49 CrossRef Medline
13. Seewann A, Kooi EJ, Roosendaal SD, et al. **Postmortem verification of MS cortical lesion detection with 3D DIR.** *Neurology* 2012;78: 302–08 CrossRef

14. Geurts JJG, Roosendaal SD, Calabrese M, et al; MAGNIMS Study Group. **Consensus recommendations for MS cortical lesion scoring using double inversion recovery MRI.** *Neurology* 2011;76:418–24 CrossRef
15. Patel S, Gershon A, Dimaandal I, et al. **Double inversion recovery to detect cervical spinal cord multiple sclerosis lesions.** *J Neuroimaging* 2023;33:521–26 CrossRef Medline
16. Riederer I, Karampinos DC, Settles M, et al. **Double inversion recovery sequence of the cervical spinal cord in multiple sclerosis and related inflammatory diseases.** *AJNR Am J Neuroradiol* 2015;36:219–25 CrossRef Medline
17. Emorine T, Megdiche I, Brugières P, et al. **3-Dimensional fluid and white matter suppression magnetic resonance imaging sequence accelerated with compressed sensing improves multiple sclerosis cervical spinal cord lesion detection compared with standard 2-dimensional imaging**. *Invest Radiol* 2022;57:575–84 CrossRef Medline
18. Xie Y, Tao H, Li X, et al. **Prospective comparison of standard and deep learning–reconstructed turbo spin-echo MRI of the shoulder**. *Radiology* 2024;310:e231405 CrossRef
19. Almansour H, Herrmann J, Gassenmaier S, et al. **Deep learning reconstruction for accelerated spine MRI: prospective analysis of interchangeability.** *Radiology* 2023;306:e212922 CrossRef
20. Kim E, Cho H-H, Cho SH, et al. **Accelerated synthetic MRI with deep learning–based reconstruction for pediatric neuroimaging**. *AJNR Am J Neuroradiol* 2022;43:1653–59 CrossRef Medline
21. Yoo H, Yoo RE, Choi SH, et al. **Deep learning–based reconstruction for acceleration of lumbar spine MRI: a prospective comparison with standard MRI**. *Eur Radiol* 2023;33:8656–68 CrossRef Medline
22. Herrmann J, Gassenmaier S, Keller G, et al. **Deep learning MRI reconstruction for accelerating turbo spin echo hand and wrist imaging: a comparison of image quality, visualization of anatomy, and detection of common pathologies with standard imaging.** *Academic Radiol* 2023;30:2606–15 CrossRef
23. Herrmann J, Koerzdoerfer G, Nickel D, et al. **Feasibility and implementation of a deep learning MR reconstruction for TSE sequences in musculoskeletal imaging.** *Diagnostics* 2021;11:1484 CrossRef
24. Dubey D, Pittock SJ, Krecke KN, et al. **Clinical, radiologic, and prognostic features of myelitis associated with myelin oligodendrocyte glycoprotein autoantibody.** *JAMA Neurol* 2019;76:301–09 CrossRef Medline
25. Loos J, Pfeuffer S, Pape K, et al. **MOG encephalomyelitis: distinct clinical, MRI and CSF features in patients with longitudinal extensive transverse myelitis as first clinical presentation.** *J Neurol* 2020; 267:1632–42 CrossRef Medline